Micron-Scale Positioning of Features Influences the Rate of Polymorphonuclear Leukocyte Migration

Jian Tan, Hong Shen, and W. Mark Saltzman
School of Chemical Engineering, Cornell University, Ithaca, New York 14853 USA

ABSTRACT Microfabrication technology was used to create regular arrays of micron-size holes (2 μm $\times$ 2 μm $\times$ 210 nm) on fused quartz and photosensitive polyimide surfaces. The patterned surfaces, which possessed a basic structural element of a three-dimensional (3-D) network (i.e., spatially separated mechanical edges), were used as a model system for studying the effect of substrate microgeometry on neutrophil migration. The edge-to-edge spacing between features was systematically varied from 6 μm to 14 μm with an increment of 2 μm. In addition, collagen was used to coat the patterned quartz surfaces in an attempt to change the adhesive properties of the surfaces. A radial flow detachment assay revealed that cell adhesion was the strongest on the quartz surface ($\sim$50% cell attached), whereas it was relatively weaker on polyimide and collagen-coated quartz ($\sim$25% cell attached). Cell adhesion to each substrate was not affected either by the presence of holes or by the spacing between holes. A direct visualization assay showed that neutrophil migration on each patterned surface could be characterized as a persistent random walk; the dependence of the random motility coefficient (μ) as a function of spacing was biphasic with the optimal spacing at $\sim$10 μm on each substrate. The presence of evenly distributed holes at the optimal spacing of 10 μm enhanced μ by a factor of 2 on polyimide, a factor of 2.5 on collagen-coated quartz, and a factor of 10 on uncoated quartz. The biphasic dependence on the mechanical edges of neutrophil migration on 2-D patterned substrate was strikingly similar to that previously observed during neutrophil migration within 3-D networks, suggesting that microfabricated materials provide relevant models of 3-D structures with precisely defined physical characteristics. In addition, our results demonstrate that the microgeometry of a substrate, when considered separately from adhesion, can play a significant role in cell migration.

INTRODUCTION

The ability of a cell to migrate is important in many physiological and pathological events; therefore, the mechanisms for cell migration have been extensively studied. Many cellular activities are mediated by chemical interactions between receptors on cell membranes and specific binding domains in extracellular matrix (ECM), which is a three-dimensional (3-D) network within tissues. But geometrical and physical properties of the ECM must also be important in regulating cell migration. Based primarily on studies of cells migrating on flat surfaces, the physical events that produce cell migration have been described as a series of steps: 1) cell membrane extension to form lamellipodia, 2) cell adhesion to substratum, 3) cytoskeletal contraction, and 4) detachment of cell membrane at rear (Palecek et al., 1999). The speed of cell migration depends on the integration of the rates of all these processes, although one step can be rate determining under certain conditions. Much information about adhesion-mediated cell migration has been obtained at the molecular level, but little is known about the influence of the physical properties of a substrate on the speed of cell migration. This information would provide insight into the mechanisms of cell migration and could also guide the design of biomaterials that interact with tissue cells.

The physicochemical properties of the environment potentially play an important role in cell migration. A frequently cited example is the adhesive property of a substrate. On a highly adhesive substrate, the overall cell-substratum bond is strong, causing a very slow rate of cell detachment (step 4 above) with the result that cells become immobilized. Conversely, on a poorly adhesive substrate, cell-substratum interaction (step 2 above) is too weak and cells cannot generate enough traction for forward migration (Palecek et al., 1999). Therefore, it is postulated that maximal speed can be obtained by cells moving on surfaces at an intermediate attachment strength (DiMilla et al., 1993). In addition to adhesiveness, other features of a material have also been identified as important determinants of speed of cell migration, such as the mechanical strength of a substrate (Kuntz and Saltzman, 1997), mesh size of a 3-D network (Kuntz and Saltzman, 1997; Mandeville et al., 1997) and topography of a 2-D surface (Haston et al., 1982). However, quantitative and systematic studies of the effect of any individual factor on cell motility are lacking, primarily due to difficulty in designing experimental systems that isolate only one of these variables.

Several lines of evidence suggest that spacing of mechanical obstacles is a critical parameter in cell motile speed. Early chemotaxis studies using Boyden chamber assays demonstrated that the speed of cell movement was influenced by the pore size of the membrane (Tucker et al., 1992; Stein et al., 1983; Smith et al., 1982; Strzemienski et al.,

Received for publication 1 September 2000 and in final form 18 June 2001.
Address reprint requests to Dr. W. Mark Saltzman, School of Chemical Engineering, 120 Olin Hall, Cornell University, Ithaca, NY 14853. Tel.: 607-255-2657; Fax: 607-255-1136; E-mail: saltzman@cheme.cornell.edu.

0006-3495/01/11/2569/11 $2.00

1987). Tumor cell migration through fibrin clots was stimulated by hyaluronan, presumably due to hyaluron's effect on fiber size and porosity (Hayen et al., 1999). The extent of tumor cell invasion into Matrigel on gelatin-coated filters was proportional to filter size and inversely proportional to the Matrigel concentration (Amar et al., 1994). Lymphocytes migrated into serum-coated micropore filters with pore sizes of 3 or 8 μm but could not attach to, or migrate into, filters made of the identical material with smaller pores (0.22 or 0.45 μm) (Haston et al., 1982). Neutrophil migration was enhanced on polycarbonate membranes containing 0.8-μm pores as compared with smooth ones (Mandeville et al., 1997).

Three-dimensional materials support cell migration through mechanisms that do not exist on a flat, two-dimensional surface. Neutrophils did not move on 2-D collagen-coated surfaces due to weak adhesion but rapidly penetrated into 3-D collagen gels (Brown, 1984). Similarly, lymphocytes did not migrate on 2-D surfaces coated with serum protein or fibronectin but were able to move effectively in hydrated 3-D collagen lattices (Haston et al., 1982). The morphology of leukocytes in a 3-D structure appears to be different from that on a 2-D surface (Grinnell, 1982): many small pseudopods are present on cells in the 3-D matrix. It has been suggested that these pseudopods can insert into gaps in the matrix and serve as anchorage points to pull the cell body (Haston et al., 1982; Brown, 1984; Mandeville et al., 1997). Recently, quantitative studies of neutrophil migration in 3-D collagen gels have demonstrated that the rate of cell migration is dependent on mesh size, which was varied by changing gel concentration or by introducing other ECM proteins (Parkhurst and Saltzman, 1992; Kuntz and Saltzman, 1997). An optimal mesh size of $\sim$7 μm, a value close to the cell diameter, was required to reach maximal speed. However, interpretation of these results was difficult due to the strong coupling between changes in gel structure and gel chemistry: it was impossible to make a graded change in structures without also affecting adhesiveness or deformability of the gels (Tan and Saltzman, 1999). Therefore, we have employed microfabrication techniques to generate physical features on different substrates that bear some analogy to the structure of a 3-D fibrous gel: spatially separated edges that provide opportunities for cells to have mechanical interactions. The feature size, shape, and distribution on a surface can be precisely controlled and individually varied over a wide range with microfabrication technology (Tan et al., 2000).

The versatility of microfabrication technology in creating precise surface structures makes it an excellent tool for studying biomedical systems (Hoch et al., 1996). Most researchers have focused on the use of chemical patterns to regulate cell behaviors (Clark et al., 1992; Mrksich et al., 1996; Corey et al., 1997; Tai and Buettner, 1998; Stenger et al., 1998; Patel et al., 1998; DeFife et al., 1999) with only a few studies using physical patterns (Rich and Harris, 1981; Clark et al., 1990; Meyle et al., 1993; Craighead et al., 1998; Brunette and Chehroudi, 1999). However, dramatic effects of physical patterns have been observed. For example, when challenged by single steps, fibroblasts and chicken embryonic neural cells were gradually inhibited from crossing steps of increasing height (1–10 μm) (Clark et al., 1987) whereas neutrophils were relatively unaffected by 5-μm steps (Clark et al., 1987). In a previous report, we created regular arrays of micron-size pillars and holes spaced at 10 μm on glass surfaces using photosensitive polyimide (PSPI) for studies of neutrophil behaviors (Tan et al., 2000). We found that neutrophil morphology, adhesion, and motility were dramatically changed by the presence of these physical features (Tan et al., 2000).

PSPI is a dual-purpose polymer that can be used either as a permanent material or as a temporary material during processing (Bureau and Droguet, 1996). Because of its excellent chemical and thermal stability and strong adherence to various substrates, polyimide has recently attracted attention as a biomaterial for use in implantable devices (Richardson et al., 1993; Akin et al., 1999; Kawakami et al., 1997; Wessa et al., 1999). In this study, regular arrays of holes were again microfabricated using PSPI. In addition, geometrically identical micro-patterns were created on substrates with different adhesive properties: quartz and collagen-coated quartz. The spacing between holes was systematically varied in the range from 6 μm to 14 μm, while the feature size was kept constant. The structural properties of micro-patterned surfaces were characterized using scanning electron microscopy (SEM) and atomic force microscopy (AFM). The adhesion of human neutrophils, the important cells in inflammatory reactions, to each substrate was measured using a radial flow detachment assay (RFDA) (Cozens-Roberts et al., 1990). The migration of live neutrophils was studied on each patterned surface using a direct visual assay. Because the patterned surfaces mimic one basic structural element of a 3-D fibrous gel, the present study can help bridge our current understanding of cell behaviors on 2-D surfaces and 3-D networks. To aid in this process, we propose a conceptual model to describe the dependence of cell motility on certain physicochemical properties of a substrate: namely, adhesiveness (which depends on chemical interactions and, therefore, angstrom-scale structure) and spacing between mechanical edges (which depends on micron-scale structure).

MATERIALS AND METHODS

Microfabrication of polyimide pillars and holes on glass substrate

PSPI was patterned using standard photolithography techniques at the Cornell Nanofabrication Facility (CNF). First, patterns were designed in CAD and transferred to a GCA PG 3600F optical pattern generator, which exposed the images of patterns on chrome masks. After development of the photoresist and wet etching of unprotected Cr, the patterns were created on

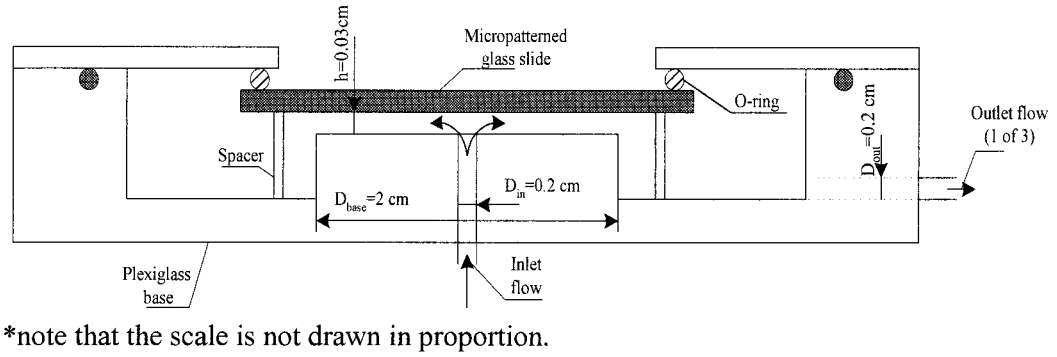

FIGURE 1 Schematic of the radial flow chamber for measurement of cell adhesion.

masks. In this study, regular arrays of squares of 2 × 2 μm were patterned, and the space between each square (edge-to-edge) in patterns differed from 6 to 14 μm at an increment of 2 μm.

The patterns of holes were created as previously described (Tan et al., 2000). Microscope slides (25 × 75 × 1 mm, VWR, West Chester, PA) were cut into three 25- × 25-mm squares and cleaned with Nanostrip (Cyantek Corp., Fremont, CA) and oxygen plasma (Plasma Therm 72). Photosensitive Probimide Polyimde 7005 (Olin Microelectronic Materials, Norwalk, CT) was spun on glass at 3000 or 5000 rpm for 30 s to obtain the desired film thickness, ~7 or 5 μm, respectively. The light yellow film was soft-baked in a 90°C convective oven for 15 or 7 min for different thicknesses to remove the solvent from the film slowly and evenly. Each film was carefully examined for its quality using optical microscopy before exposure. GCA 6300 10:1 i-line stepper was use to expose the film, and the film was immediately baked at 90°C for 5 min. The exposed area was cross-linked and insoluble; the unexposed regions remained soluble and were washed away during development with Olin QZ 3501/QZ3512. To convert the Probimide photosensitive polyimide precursor into polyimide, the patterns were cured in a nitrogen-gas-purged oven at 350°C for 1 h (Yield Engineering System Polyimide oven). The final product was brown and transparent with a reduced film thickness of 4.5 or 2.5 μm.

Microfabrication of holes in fused quartz surfaces

Fused quartz chips (25 × 25 × 1 mm, Quartz Scientific, Fairport Harbor, OH) was cleaned with Chromerge (chromic-sulfuric acid, EM Science, Fort Washington, PA) and oxygen plasma (Plasma Therm 72) and vapor-primed with hexamethyldisilazane (HMDS) to increase adhesion. Next, photoresist (OCG OiR 897–12i) was spun on the chips and soft-baked at 90°C on a hot plate for 90s. Then, the chips were exposed through a Cr mask using 10:1 i-line stepper and post-exposure baked at 115°C for 120s. The photoresist was developed in Shipley CD-26 for 60s. The patterned quartz chips were etched in PT72 using gas mixture CHF_3/O_2 for 15 min.

Characterization of micropatterned surfaces

The chips were coated with Au-Pd and examined by a high-magnification SEM (Zeiss LEO2, DSM 982 field emission scanning electron microscope) at a low voltage (<5 kev). Because it was difficult to measure the depth of holes with SEM, the surfaces with holes were scanned at a rate of 1 Hz by atomic force microscopy (AFM Digital Instruments 3100 AFM) using tapping mode. The depth of holes was then measured using section analysis.

Neutrophil separation

Neutrophils were separated and purified by a method described previously (Tan and Saltzman, 1999). Whole blood from healthy donors was collected by venipuncture into vials containing heparin. About 7 ml of the blood was layered onto 4 ml of mono-poly resolving media (ICN Flow, Irvine, CA) and centrifuged at 1700 rpm (490 × g) for 30 min. The lower band of white cells was transferred into a clean tube and underlayered with 1 ml of fresh mono-poly resolving media. The tube was centrifuged at 2900 rpm (1440 × g) for 15 min to remove residual erythrocytes. The upper fraction was collected and cells were washed twice with serum-free medium M199 before being resuspended in the medium to the desired concentration.

Collagen coating of quartz chips patterned with regular arrays of holes

The patterned chips (cut into four pieces from original ones) were placed in a 12-well tissue culture plate and coated with 1 ml/well collagen solution (Vitrogen 100, Cohesion, Palo Alto, CA) that was diluted to 40 μg/ml in M199 medium overnight at room temperature. The chips were rinsed with M199 three times before use for adhesion or motility studies. This method should generate a thin coating of collagen on the quartz surface, not a gel type or fibrillar structure (Brown, 1982). The coated chips were examined under SEM to confirm no fiber formation.

Cell adhesion to micropatterned surfaces using radial flow detachment assay

A schematic of the flow chamber for radial flow detachment assay (RFDA) is shown in Fig. 1 (Cozens-Roberts et al., 1990). The flow chamber consisted of 1) an upper micropatterned glass slide (25 × 25 × 1 mm), 2) a lower cylindrical Plexiglas base with an inlet hole at the center of the disc, 3) four Plexiglas spacers used to separate the micropatterned glass slide and the Plexiglas base, 4) an upper Plexiglas cover plate (9 cm × 0.3 cm) with a 1.5-cm hole at the center of the plate, and 5) two Viton O-rings (Scientific Instruments Services, Ringoes, NJ) used to provide a good seal between the cover plate and the base. Outlet flow was through three 0.2-cm holes in the wall of the lower Plexiglas disc. This flow chamber produced a well-defined axisymmetric laminar shear flow between the micropatterned chips and the Plexiglas cylindrical base separated by a gap of height h = 0.03 cm when the volumetric flow rate is 1.1 ml/s.

The measurement of cell adhesion was carried out at room temperature. Neutrophils at a density of 2.5 × 10^4 cell/cm^2 were allowed to settle on clean micropatterned chips for 15 min in the presence of M199. The slide was rinsed very gently using a pipette to wash away nonadherent cells.

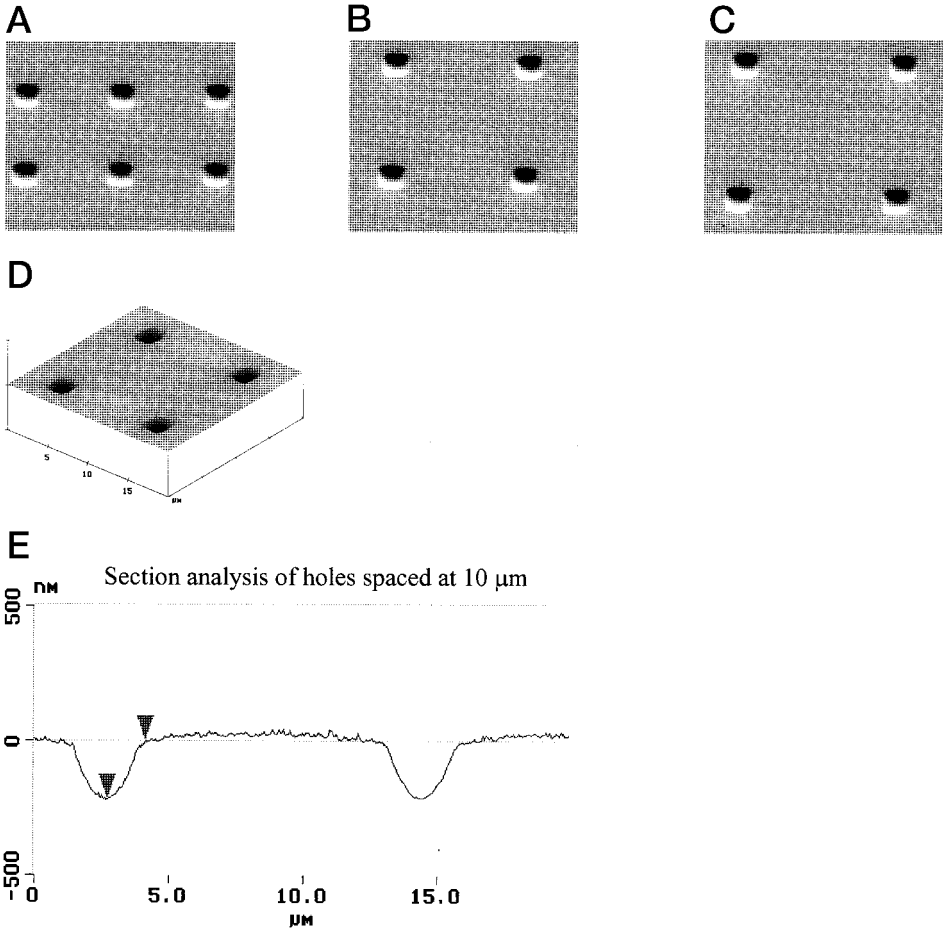

FIGURE 2 (*a–c*) SEM images of microfabricated polyimide surfaces with holes (2 μm × 2 μm × 210 nm) spaced at 6 μm (*a*), 10 μm (*b*), and 14 μm (*c*); (*d*) AFM images of holes spaced at 10 μm; (*e*) Section analysis of holes spaced at 10 μm.

Four fields with the same size were selected at the same radial position of 2.3 mm, and pictures were taken to record the number of cells before the flow. The micropatterned chips were carefully assembled in the flow chamber that was filled with PBS. The center of chips was in the center of the inlet flow. Next, the flow chamber was connected to a head tank containing PBS. The flow rate was maintained at a constant value of 1.1 ml/s. The chip was removed from the flow chamber after 20 min of steady flow, and pictures of the pre-selected areas were taken immediately to determine the number of remaining cells. The experiments were repeated four times for each of at least five donors, and the average percentage of adherent cells under each condition was determined.

Cell motility on micropatterned surfaces using direct visual assay

The details of this method have been published previously (Parkhurst and Saltzman, 1992; Tan et al., 2000). Micropatterned surfaces were used after rinsing with de-ionized water and blow-drying with 0.22-μm-filtered air. Control experiments were performed on smooth areas (no pattern) of polyimide, quartz, and collagen-coated quartz. About 75 μl of neutrophils at a concentration of 2×10^5 cells/ml was added onto the surface resulting in a cell density of 1.5×10^4 cells/cm^2. Cells were allowed to settle on the substrate in a cell culture plate at 37°C for 15 min before the plate was placed on the stage of an inverted light microscope (Diaphot, Nikon, Garden City, NY). An incubator surrounding the stage was preheated and maintained at 37 ± 0.5°C throughout the experiment. Cell movement on the substrate was monitored by a computer-based image analysis system (NIH Image 1.61). Digitized still images of the field of view were collected every 90 s for 15 min. The positions of cells were determined on each digitized image by tracing the cell outline and calculating the center of mass. This procedure produced an x, y record of cell position on each frame, with positioning error less than 1 μm. Each experiment was performed with a variety of donors (at least five) to examine a large population of cells. The square displacement of 60–100 cells was calculated for every possible time interval, and the mean squared displacement as a function of time was described using the following equation:

$$D^2(t) = 4\mu(t - P + Pe^{-t/P}), \quad (1)$$

where $D^2(t)$ is the mean squared displacement over a time interval of length t, μ is the random motility coefficient, and P is the persistence time. When time is sufficiently large, $t \gg P$, Eq. 1 reduces to $D^2(t) = 4\,\mu\,(t - P)$. The values for μ and P were estimated from the slope and intercept of this line. Because large errors could be associated with the estimation of P using this method, we did not attempt to analyze the results of persistence time.

RESULTS

In our previous studies, we demonstrated that the motility of neutrophils was greatly enhanced by micropatterned holes on polyimide surfaces with a spacing of 10 μm whereas it was significantly decreased by pillars arranged with the same spacing (Tan et al., 2000). In this study, we focused our investigation of cell motility on different surfaces with identical patterns of holes.

TABLE 1 Depth (nm) of holes measured by AFM

	Film thickness (μm)	
Spacing (μm)	2.5	4.5
6	214 ± 8	207 ± 10
10	214 ± 9	217 ± 3
14	218 ± 5	220 ± 5

Microfabrication and characterization of surfaces micropatterned with holes

Regular arrays of holes (Fig. 2, *a*—*c*; only 6-, 10-, and 14-μm spacing are shown for simplicity) were first successfully fabricated in polyimide film that was spun on glass surfaces using standard photolithography. Each hole was a 2 × 2 μm square and the spacing between them was varied from 6 to 14 μm with an increment of 2 μm as defined. We intended to vary the depth of holes by changing the film thickness, although the desired depth of holes was not obtained; they appeared rather shallow in SEM pictures. AFM was used to scan all the holes made in both 2.5-μm- and 4.5-μm-thick polyimide films. A typical AFM image of holes with a spacing of 10 μm is shown in Fig. 2 *d*. Section analysis in AFM was used to measure the depth of holes in both films (Table 1). The depth of holes was constant at various spacing with a value of only ~210 ± 10 nm; surprisingly, it was also independent of film thickness ($p < 0.01$). This finding suggests that a similar surface structure was created with this pattern design, regardless of the film thickness of polyimide. The effect could be due to the limitation in depth of focus (~1 μm) during exposure using 10× projection lithography. Even though the desired depth of holes was not obtained, the results of SEM and AFM studies showed that it was possible to change the spacing between features while keeping the other parameters constant using microfabrication techniques.

Similar patterns were produced on fused silica substrates. The size of holes was kept constant at 2 μm × 2 μm; the spacing between holes was again varied from 6 μm to 14 μm with an increment of 2 μm (Fig. 3, *a*—*c*; only 6-, 10-, and 14-μm spacing are shown for simplicity). The depth of holes in quartz was easily controlled by varying the etching time in PT72. To be consistent with the pattern in polyimide, the time for etching quartz was adjusted to obtain the same depth (210 nm) as that obtained with polyimide; AFM was used to confirm the desired depth.

After optimization of the process for each pattern on both polyimide and fused quartz, identical copies of the structures were produced in large quantity for studying cell motility. Some of the patterned quartz chips were coated with collagen before cell experiments.

Neutrophil adhesion to micropatterned surfaces with holes

Previously, we used a centrifugation assay to compare the adhesive properties of patterned surfaces (Tan et al., 2000). After applying a mild centrifugal force (28 × *g*), no neutrophils were attached to polyimide surfaces with or without holes, whereas about half of the cells remained on glass and pillared surfaces. To achieve a wider range of detachment forces, and to allow for better comparison of cell adhesion to various substrates, we adopted a RFDA method (Cozens-Roberts et al., 1990). The percentage of the remaining cells on the surfaces after applying a fixed hydrodynamic shear force was used to indicate the strength of cell-substratum attachment. Plain quartz surfaces, which retained 50% of pre-attached cells, were much more adhesive to neutrophils than smooth polyimide films and collagen-coated quartz, which retained about the same amount, only 25%. On each substrate, cell adhesion on areas of the surfaces with holes was identical to unpatterned areas ($p > 0.03$), and the spacing between holes did not affect cell adhesion (Fig. 4).

Cell migration on surfaces micropatterned with holes

Polyimide surface

Many cells were able to migrate significant distances on the patterned surfaces through dynamic membrane extensions, as seen by direct visualization. Typical paths of cell movements on surfaces with holes spaced at 10 μm are depicted in Fig. 5 *a*. The motion of neutrophils was characterized as a persistent random walk (Tan et al., 2000); for example, the mean squared displacement (D^2) of movement for a popu-

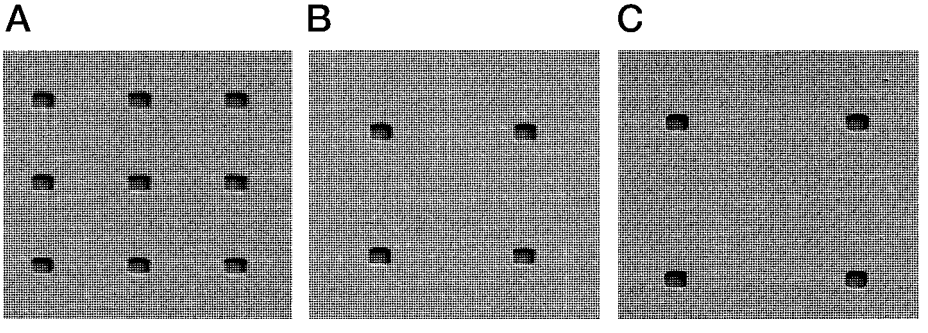

FIGURE 3 SEM images of microfabricated quartz surfaces with holes (2 μm × 2 μm × 210 nm) spaced at 6 μm (*a*), 10 μm (*b*), and 14 μm (*c*).

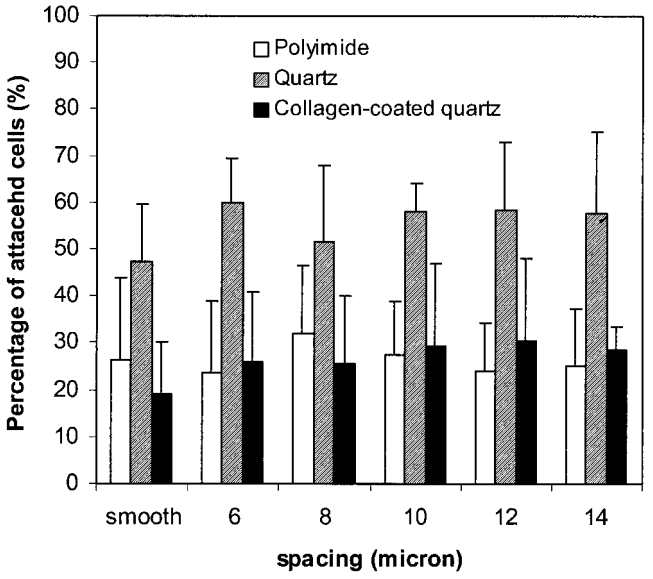

FIGURE 4 Neutrophil adhesion to surfaces with varied surface chemistry and microgeometry.

lation of cells on patterned polyimide films of 4.5 μm thickness is plotted as a function of time (Fig. 6 *a*). $D^2(t)$ was linear with time, after the initial lag period, so that the random motility coefficients, μ, could be determined (Table 2). The random motility coefficient for both 4.5- and 2.5-μm-thick films as a function of spacing was similar (Fig. 6 *b*). This result was consistent with the finding from AFM examination, in which the microgeometry of patterned holes in two films with different thickness was essentially the same. On the other hand, the result also indicated that surface roughness and other physicochemical properties that might be changed during spin-coating at different speed were not important.

The dependence of motility on the spacing between holes can be described as biphasic with the maximal motility occurring at 10 μm: 3.6×10^{-9} and 3.5×10^{-9} cm^2/s for 2.5- and 4.5-μm-thick films respectively. When the spacing was changed to either 8 or 12 μm (i.e., only 2 μm from the optimal spacing), the cell motility coefficient dropped to $\sim 2.4 \times 10^{-9}$ cm^2/s on 4.5-μm-thick film, and $\sim 2.3 \times$

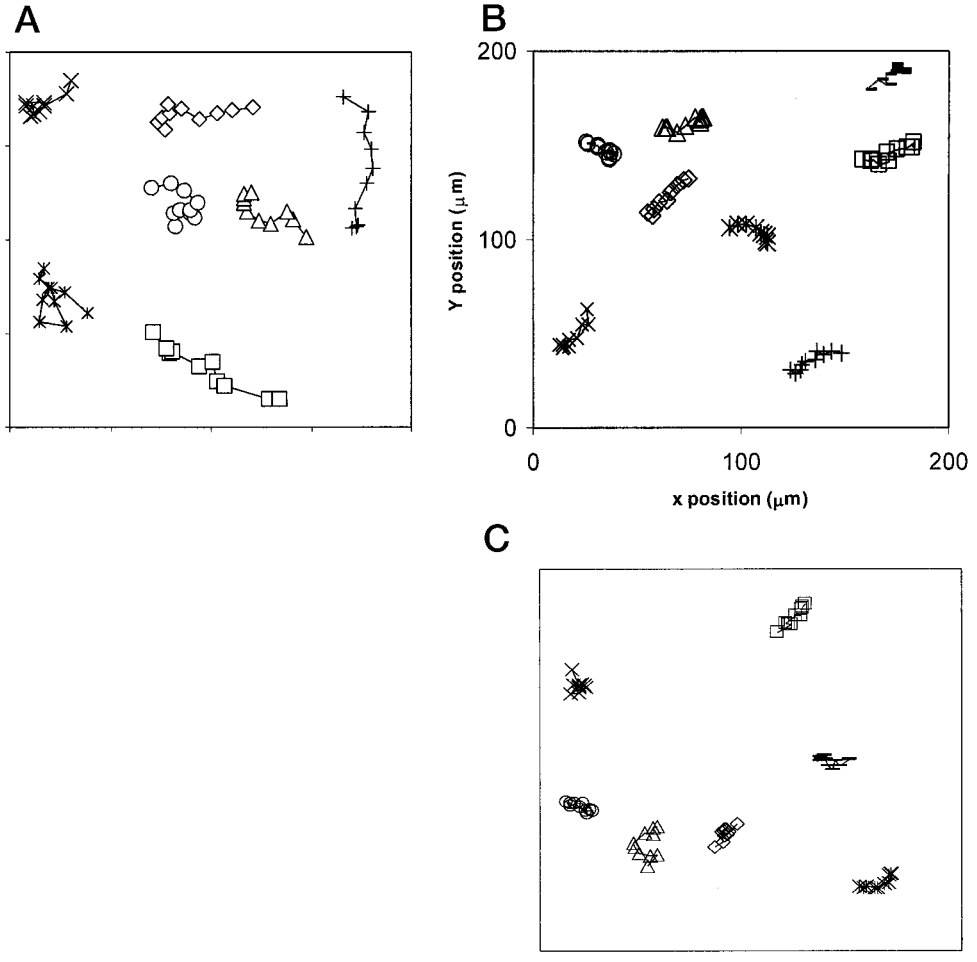

FIGURE 5 Typical paths of neutrophils on surfaces patterned with holes spaced at 10 μm: polyimide (*a*), collagen-coated quartz (*b*), and quartz (*c*), which are characterized as persistent random walk.

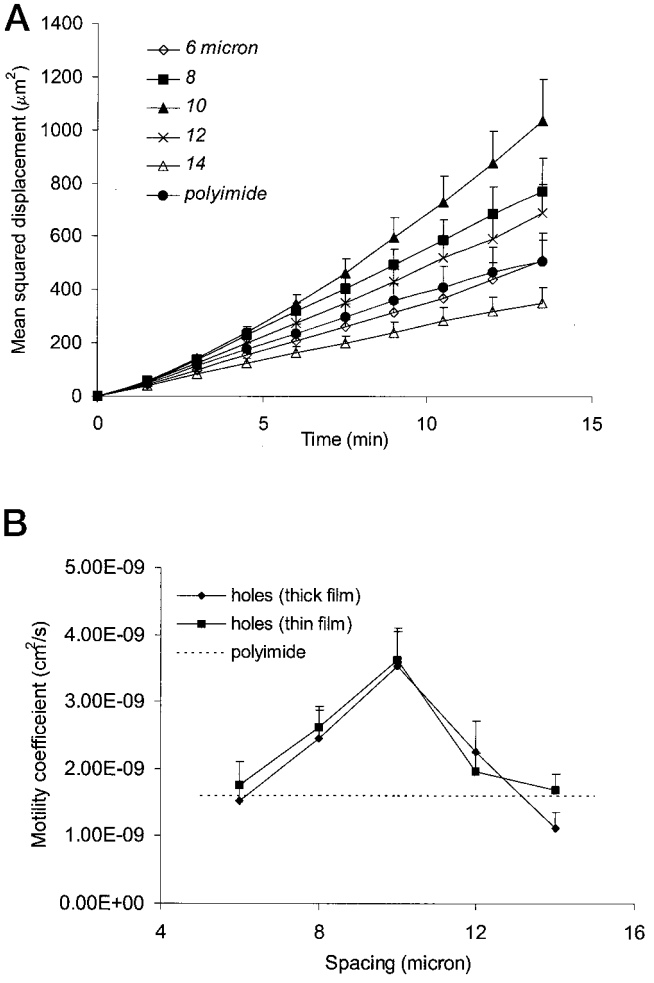

FIGURE 6 Influence of spacing between holes on neutrophil migration on polyimide surfaces. (*a*) Mean squared displacement as a function of time; (*b*) Random motility coefficients as a function of spacing; ·····, motility coefficient of cells on unpatterned surface.

10^{-9} cm^2/s on 2.5-μm-thick film, respectively. When the spacing was further changed to 6 and 14 μm, the motility on patterned surface was reduced further to a value similar to that on smooth polyimide surface (1.6×10^{-9} cm^2/s).

TABLE 2 Random motility coefficient μ estimated from plots of mean square displacement as a function of time

Spacing (μm)	Polyimide (10^{-9} cm^2/s)		Quartz (10^{-10} cm^2/s)	
	a = 2.5 μm	a = 4.5 μm	No coating	Collagen coated
6	1.8 ± 0.4	1.5 ± 0.3	3.2 ± 0.7	4.1 ± 0.9
8	2.6 ± 0.3	2.5 ± 0.4	2.9 ± 0.9	5.2 ± 1.1
10	3.6 ± 0.4	3.5 ± 0.5	3.7 ± 0.8	8.5 ± 1.3
12	2.0 ± 0.3	2.3 ± 0.4	1.7 ± 0.4	6.6 ± 1.5
14	1.7 ± 0.2	1.1 ± 0.2	1.8 ± 0.4	5.8 ± 1.0
No pattern	1.6 ± 0.4		0.3 ± 0.1	3.0 ± 1.1

Please note the unit of μ was different for polyimide and quartz substrates. *a*, thickness of the film in which holes were made; the actual depth of holes was much smaller at ~210 nm measured by AFM.

Probably because of the uncertainty in the estimation of P by this procedure, which has also been identified in previous work (Parkhurst and Saltzman, 1992), we found no correlation in variations of P with surface characteristics.

Fused quartz surface

Cell movement was extremely slow on uncoated quartz; most cells were almost immobilized on smooth area without any holes, even though they demonstrated rapid membrane extensions. In the presence of holes, cells could migrate for short distances (Fig. 5 *c*). The movement of the cells was analyzed identically to that on polyimide surfaces. Motility coefficient μ was only 3×10^{-11} cm^2/s (Table 2), ~50 times slower than that on smooth polyimide surface. Cell motility was significantly increased (~5–12-fold) on each patterned surface with holes of different spacing; however, relatively large errors were associated with μ as compared with the values obtained on polyimide. Again, the maximal μ, 3.7×10^{-10} cm^2/s, was also observed at a spacing of 10 μm (Table 2), but the motility coefficient did not change as dramatically with spacing on quartz (Fig. 7 *b*). Cell motility only decreased slightly when the spacing was changed to 6 or 8 μm, 3.2×10^{-10} and 2.9×10^{-10} cm^2/s, respectively; it dropped sharply to a value of 1.7×10^{-10} cm^2/s when the spacing was increased to 12 μm. Further increase in spacing to 14 μm did not change cell motility, with μ at 1.8×10^{-10} cm^2/s.

Collagen-coated fused quartz surface

Because neutrophils strongly attached to quartz surfaces, resulting in very slow motility, bovine dermal collagen was coated on the patterned quartz chips to change the adhesive property of the substrate. SEM examination confirmed that the coating was monomeric; e.g., collagen fibers did not form on the surfaces. Cell migration on both non-patterned and patterned surfaces was increased markedly (Fig. 5 *b*). Collagen coating increased the motility on unpatterned quartz surfaces by 10 times over uncoated ones, a baseline μ at 3.0×10^{-10} cm^2/s (Table 2). The presence of holes further increased cell motility, and the effect of spacing was again biphasic (Fig. 8 *b*). The maximal μ, 8.5×10^{-10} cm^2/s, was obtained at a spacing of ~10 μm. A drop in motility coefficient occurred when the spacing was decreased to 8 or 6 μm, 5.2×10^{-10} and 4.1×10^{-10} cm^2/s. A relatively mild drop was obtained when spacing was increased to 12 and 14 μm, 6.6×10^{-10} and 5.8×10^{-10} cm^2/s, respectively.

DISCUSSION

Both chemical and physical properties of the extracellular environment significantly affect cell motility. It is well known that specific chemical interactions between cell sur-

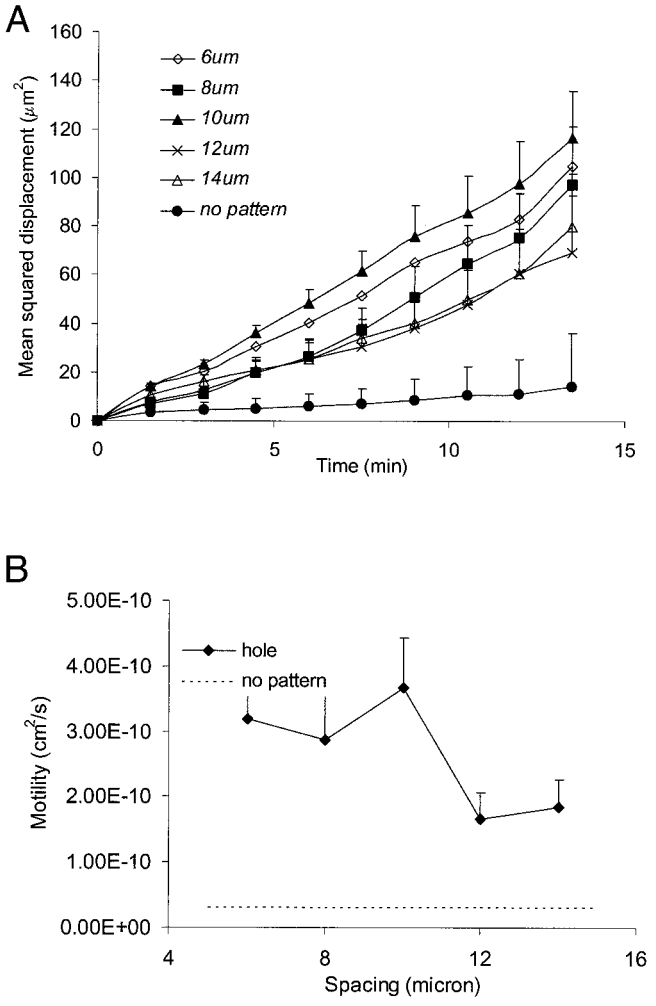

FIGURE 7 Influence of spacing between holes on neutrophil migration on quartz surfaces. (*a*) Mean squared displacement as a function of time; (*b*) Random motility coefficients as a function of spacing. · · · · ·, motility coefficient of cells on unpatterned surface.

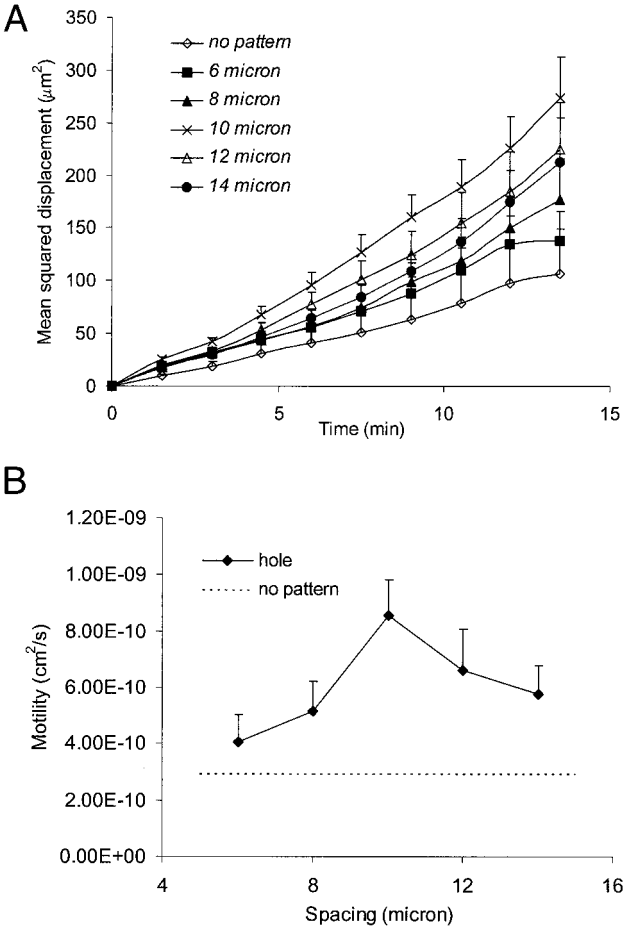

FIGURE 8 Influence of spacing between holes on neutrophil migration on collagen-coated quartz surfaces. (*a*) Mean squared displacement as a function of time; (*b*) Random motility coefficients as a function of spacing. · · · · ·, motility coefficient of cells on unpatterned surface.

face receptors and ligands attached to a substrate can trigger cellular machinery for migration and influence cell adhesion. But physical properties, including the mechanical strength, architecture, and general adhesive nature of the substrate, can also contribute significantly to cell motility under a range of conditions (DiMilla et al., 1993; Kuntz and Saltzman, 1997; Tan and Saltzman, 1999). However, it has been difficult to single out the contribution of an individual physical factor to the migration process due to the difficulty in changing one physical element without affecting the others. With the use of microfabrication technology, we were able to make new materials in which only one of the physical properties was varied. Simple patterns, regular arrays of holes, were created on surfaces to mimic the most basic structural elements of a 3-D gel. The motility on smooth surfaces was dependent on the chemical properties of the substrate; motility on collagen-coated quartz was greater than motility on polyimide, which was greater than motility on quartz (Table 2). But cell motility was also significantly enhanced by addition of properly distributed holes with an optimal spacing; the optimal spacing was 10 μm on all of the substrates. These findings demonstrate that the microgeometry of a substrate plays a significant role in cell migration, which can be separated from the effect of chemical adhesion.

Cell-substratum adhesion is an important parameter in the determination of cell speed. Stationary cells tend to form focal contacts that prevent movement, whereas mobile cells usually do not form a highly adhesive bond with a substrate (DiMilla et al., 1991). In this study, we examined cell motility on two weakly adhesive surfaces (polyimide and collagen-coated quartz) and one strongly adhesive surface (quartz). It should be noted that we used the percentage of cells remaining attached after applying an arbitrary hydrodynamic shear force as an indication of strength of cell adhesion. Therefore, the reported adhesion in this study may not reflect the complete nature and specificity of cell-sub-

stratum chemical interactions. But this simple indicator of cell adhesion allowed us to confirm that addition of certain physical patterns (such as regularly spaced, 2-μm holes) did not influence adhesion of the cell population.

Previous studies have shown that the apparent adhesive force is not the only factor that governs cell movement. For example, cell speed was faster on fibronectin-coated surfaces than on collagen-IV-coated surfaces, even though the two surfaces have the same measured overall adhesiveness (e.g., critical shear stress) (DiMilla et al., 1993). In that case, other factors (probably involving cellular activities triggered by specific chemical interactions between the cell membrane receptors and fibronectin/collagen substrate) also play important roles. In our experiments, neutrophil migration on unpatterned quartz was extremely slow ($\mu = 3.0 \times 10^{-11}$ cm^2/s), probably because cell adhesion to quartz was too strong for efficient cell detachment, leaving cells unable to move effectively. When the adhesion was decreased by means of collagen coating, cells were able to move more rapidly, exhibiting a 10-fold increase in motility coefficient. Although neutrophil adhesion to collagen-coated quartz and polyimide surfaces was similar, the motility coefficient on the two surfaces was significantly different: 3.0×10^{-10} and 1.6×10^{-9} cm^2/s. Because the surface chemistry of quartz, collagen-coated quartz, and polyimide was also significantly different, it is possible that the cellular activities triggered by the three surfaces would differ in many important ways, such as specific membrane receptor bindings, cytoskeleton reactions, etc., leading to different cell motility.

Cell adhesion to each of the substrates examined in this study was not affected either by the presence of holes or the spacing between them. This finding suggests that the microgeometry, i.e., the spacing between 2-μm holes, on a surface can be varied without the complication of changes in the observed cell attachment. Because the surface chemistry of each substrate was the same for different spacing, the cellular machinery generated from cell-substratum interaction was probably similar for substrates that were identical except for different spacing. Therefore, the changes we observed in the motility coefficient on each patterned substrate reflect the effect of an isolated physical characteristic, e.g. the spacing between holes.

Properly distributed holes led to a significant increase in cell motility on each surface with different chemistry (adhesion). For example, the motility coefficient on the polyimide surface with holes as shallow as 210 nm was more than two times greater than that on smooth surface: 3.6×10^{-9} cm^2/s at a spacing of 10 μm versus 1.6×10^{-9} cm^2/s on unpatterned polyimide. It was almost three times greater on patterned collagen-coated quartz than unpatterned collagen-coated quartz, and 10 times greater on quartz. Previous studies suggest that cell detachment is rapid on low adhesive surfaces; therefore, the speed of cell migration may be limited by lamellipod extension or formation of new adhesions (Palecek et al., 1998; Wessels et al., 1994). This appears to be the situation for neutrophil migration on patterned surfaces; cells can use the edges of holes as footholds to gain mechanical adhesion, an additional source of traction that is absent on smooth surfaces (Haston et al., 1982). Cell motility was very sensitive to the spacing between (or density of) holes; when the spacing differed from the optimal value (10 μm) by only 2 μm, cell migration slowed down by ~30% on polyimide and 20% (12 μm) or 40% (8 μm) on collagen-coated surfaces. This observation suggests that the frequency of mechanical interaction with edges on a substrate probably depend on the geographical distribution of edges. This dependence is probably more complicated when the adhesion to a substrate is strong, as indicated by our result with quartz surfaces (Fig. 7). Nevertheless, we note that the strong biphasic dependency of motility on spacing had a striking similarity to the dependence of cell migration in three-dimensional collagen gels, in which the motility coefficient was also a biphasic function of gel concentration with the greatest motility obtained at a concentration of ~0.4 mg/ml. The maximal mesh size (or interfiber spacing) for a 0.4-mg/ml collagen gel is ~7 μm (Parkhurst and Saltzman, 1992; Kuntz and Saltzman, 1997), a number that is not substantially different from the optimal spacing identified on micropatterned surfaces with holes, 10 μm. It has been estimated that the maximal interfiber spacing (δ) of a collagen gel is proportional to the inverse of the square root of concentration (Saltzman et al., 1994): $\delta \propto 1/\sqrt{conc}$. Therefore, the maximal mesh size of the collagen gels ranged from 14 μm to 5 μm as the concentration increased from 0.1 mg/ml to 0.8 mg/ml. In summary, the dependence of motility coefficient on mesh size was comparable to that observed on micropatterned surfaces with holes (Fig. 9).

It should be noted that the collagen gel system differs from our micropatterned systems in important ways: 1) the mesh size of collagen represents the average of a broad

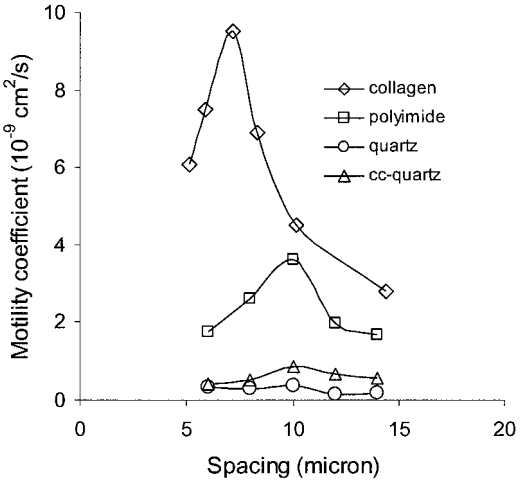

FIGURE 9 Comparison between cell motility coefficients on 2-D surfaces patterned with holes and 3-D collagen gels.

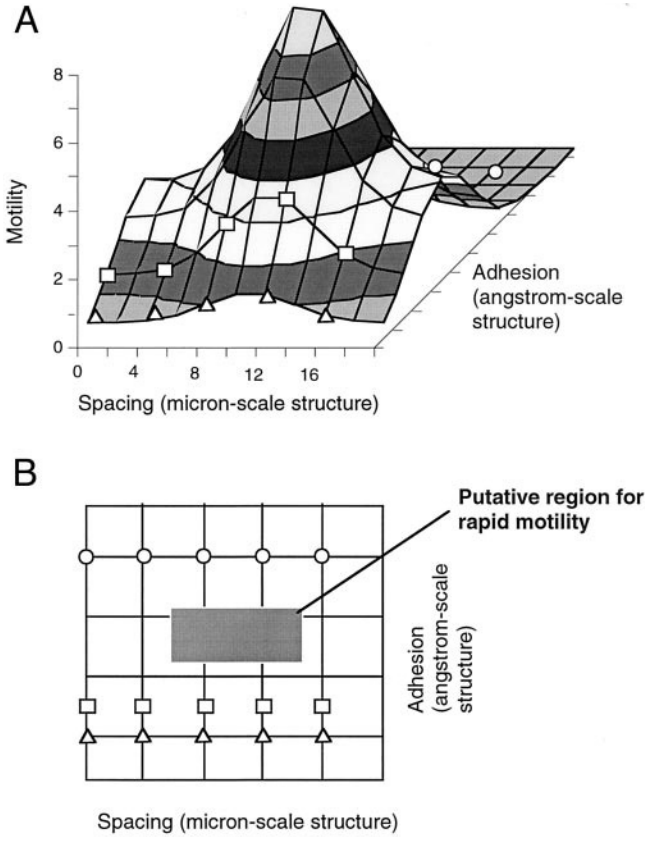

FIGURE 10 A putative model for the effect of angstrom-scale structure (which is responsible for cell adhesion and activation) and micron-scale structure (which is responsible for the spacing of obstacles) on cell motility. Symbols are added to indicate the relative positions of the measurements in this report for collagen-coated quartz (△), polyimide (□), and quartz (○). The two panels indicate a full three-dimensional view (*a*) and a top view (*b*) of the adhesion-spacing plane.

distribution of sizes, not a fixed value (Saltzman et al., 1994); 2) any changes in mesh size within the collagen also produced changes in other important parameters such as gel chemistry, adhesiveness, and mechanical strength that probably contributed to cell motility; 3) collagen fibers are deformable by the moving cells, whereas polyimide and quartz features are much stiffer. In these experiments, the chemistry, adhesiveness, and mechanical strength were purposely maintained constant so that the change in cell motility was caused by differences in only the spacing between holes. We consider the hole-patterned surface as an idealized 3-D structure, which contains precisely controlled spacing between mechanical edges but constancy of other physicochemical parameters. Mechanical edges, which provide footholds for cells to generate traction, were probably the rate-determining factor in cell migration either on micropatterned surfaces with holes or in collagen gels. We speculate that an optimal distribution of the footholds must be similar in spacing to the cell diameter, yet will depend on the other properties on individual substrate.

Based on our current knowledge, we propose a putative relationship between cell motility, the chemistry of adhesion, which depends on angstrom- or nanometer-scale interactions, and the micron-scale spacing of mechanical edges in a substrate (Fig. 10). On a smooth surface where no mechanical adhesion can be obtained, the ability of cells to migrate depends solely on chemical adhesion, i.e., a specific interaction between cell membrane and the substrate. For these systems, the dependence is usually biphasic, as has been well documented by others for cell migration on protein-coated surfaces (DiMilla et al., 1993). On a substrate with mechanical edges (either 2-D or 3-D), however, the speed of cell migration is determined by a combination of the mechanical interactions and the chemical adhesions. On substrates with low chemical adhesion, cell motility is probably determined by the available traction that can be generated from mechanical footholds; in these cases, the cell motility exhibits a biphasic dependence on spacing. We have observed this behavior by the variation in motility on polyimide and collagen-coated surfaces with holes. On highly adhesive surfaces, the traction gained from mechanical interactions can be used to overcome the strong chemical adhesion between the cell and the substrate; although the detachment rate at the cell rear probably limits cell motility, the dependence on spacing is still present. We illustrate this situation by the variation of motility on quartz surface. On optimally adhesive surfaces, we predict that cell migration will be facilitated by the both chemical and mechanical adhesion to generate a maximal motility. The simple model suggests that there may exist materials with the proper combination of angstrom-scale and micron-scale features to provide much more rapid motility than any observed in the present study (Fig. 10 *b*). This simple model may also explain the markedly slower migration (Fig. 9) on synthetic materials compared with natural materials, which have evolved features necessary to allow the efficient migration of protective neutrophils.

We thank the CNF staff for their help in microfabrication technology. We thank Katrina L. Carter and Thomas M. Yung for the help in tracking cell positions in motility study.

This work was supported by a grant from the National Science Foundation (BES-9710313) to W.M.S. and was performed in part at CNF (a member of National Nanofabrication Users Network), which is supported by the National Science Foundation under grant ECS-9319005, Cornell University, and industrial affiliates.

REFERENCES

Akin, T., B. Ziaie, S. A. Nikles, and K. Najafi. 1999. A modular micromachined high-density connector system for biomedical application. *IEEE Trans. Biomed. Eng.* 46:471–480.

Amar, A. P., S. J. DeArmond, D. R. Spencer, P. F. Coopersmith, D. M. Ramos, and M. L. Rosenblum. 1994. Development of an in vitro extracellular matrix assay for studies of brain tumor cell invasion. *J. Neurooncol.* 20:1–15.

Brown, A. 1982. Neutrophil granulocytes: adhesion and locomotion on collagen substrata and in collagen matrices. *J. Cell. Sci.* 58:455–467.

Brown, A. F. 1984. Neutrophil and monocyte behavior in three-dimesional collagen matrices. *Scan. Electron Microsc.* 2:747–754.

Brunette, D. M., and B. Chehroudi. 1999. The effects of the surface topography of micromachined titanium substrata on cell behavior in vitro and in vivo. *J. Biomech. Eng.* 121:49–57.

Bureau, J., and J. Droguet. 1996. Applications of polyimides as photosensitive materials. *In* Polyimides: Fundamentals and Applications. M. K. Ghosh and K. L. Mittal, editors. Marcel Dekker, New York.743–757.

Clark, P., P. Connolly, A. S. Curtis, J. A. Dow, and C. D. Wilkinson. 1987. Topographical control of cell behaviour. I. Simple step cues. *Development.* 99:439–48.

Clark, P., P. Connolly, A. S. Curtis, J. A. Dow, and C. D. Wilkinson. 1990. Topographical control of cell behaviour. II. Multiple grooved substrata. *Development.* 108:635–644.

Clark, P., P. Connolly, and G. R. Moores. 1992. Cell guidance by micropatterned adhesiveness in vitro. *J. Cell Sci.* 103:287–292.

Corey, J. M., A. L. Brunette, M. S. Chen, J. A. Weyhenmeyer, G. J. Brewer, and B. C. Wheeler. 1997. Differentiated B104 neuroblastoma cells are a high-resolution assay for micropatterned substrates. *J. Neurosci. Methods.* 75:91–97.

Cozens-Roberts, C., J. A. Quinn, and D. A. Lauffenburger. 1990. Receptor-mediated adhesion phenomena: model studies with the radial-flow detachment assay. *Biophys. J.* 58:107–125.

Craighead, H. G., S. W. Turner, R. C. Davis, C. James, A. M. Perez, P. M. St. John, M. S. Isaacson, L. Kam, W. Shain, J. N. Turner, and G. Banker. 1998. Chemical and topographical surface modification for control of central nervous system cell adhesion. *J. Biomed. Microdevices.* 1:49–64.

DeFife, K. M., E. Colton, Y. Nakayama, T. Matsuda, and J. M. Anderson. 1999. Spatial regulation and surface chemistry control of monocyte/macrophage adhesion and foreign body giant cell formation by photochemically micropatterned surfaces. *J. Biomed. Mater Res.* 45:148–154.

DiMilla, P. A., K. Barbee, and D. A. Lauffenburger. 1991. Mathematical model for the effects of adhesion and mechanics on cell migration speed. *Biophys. J.* 60:15–37.

DiMilla, P. A., J. A. Stone, J. A. Quinn, S. M. Albelda, and D. A. Lauffenburger. 1993. Maximal migration of human smooth muscle cells on fibronectin and type IV collagen occurs at an intermediate attachment strength. *J. Cell Biol.* 122:729–737.

Grinnell, F. 1982. Migration of human neutrophils in hydrated collagen lattices. *J. Cell Sci.* 58:95–108.

Haston, W. S., J. M. Shields, and P. C. Wilkinson. 1982. Lymphocyte locomotion and attachment on two-dimensional surfaces and in three-dimensional matrices. *J. Cell Biol.* 92:747–752.

Hayen, W., M. Goebeler, S. Kumar, R. Riessen, and V. Nehls. 1999. Hyaluronan stimulates tumor cell migration by modulating the fibrin fiber architecture. *J. Cell Sci.* 112:2241–2251.

Hoch, H. C., L. W. Jelinski, and H. G. Craighead. 1996. Nanofabrication and Biosystems. Cambridge University Press, New York.

Kawakami, H., Y. Mori, J. Takagi, S. Nagaoka, T. Kanamori, T. Shinbo, and S. Kubota. 1997. Development of a novel polyimide hollow fiber for an intravascular oxygenator. *Asaio. J.* 43:M490–M494.

Kuntz, R. M., and W. M. Saltzman. 1997. Neutrophil motility in extracellular matrix gels: mesh size and adhesion affect speed of migration. *Biophys. J.* 72:1472–1480.

Mandeville, J. T., M. A. Lawson, and F. R. Maxfield. 1997. Dynamic imaging of neutrophil migration in three dimensions: mechanical interactions between cells and matrix. *J. Leukocyte Biol.* 61:188–200.

Meyle, J., K. Gultig, H. Wolberg, and A. F. v. Recum. 1993. Fibroblast anchorage to microtextured surfaces. *J. Biomed. Mater. Res.* 27: 1553–1557.

Mrksich, M., C. S. Chen, Y. Xia, L. E. Dike, D. E. Ingber, and G. M. Whitesides. 1996. Controlling cell attachment on contoured surfaces with self-assembled monolayers of alkanethiolates on gold. *Proc. Natl. Acad. Sci. U.S.A.* 93:10775–10778.

Palecek, S. P., A. F. Horwitz, and D. A. Lauffenburger. 1999. Kinetic model for integrin-mediated adhesion release during cell migration. *Ann. Biomed. Eng.* 27:219–235.

Palecek, S. P., A. Huttenlocher, A. F. Horwitz, and D. A. Lauffenburger. 1998. Physical and biochemical regulation of integrin release during rear detachment of migrating cells. *J. Cell Sci.* 111:929–940.

Parkhurst, M. R., and W. M. Saltzman. 1992. Quantification of human neutrophil motility in three-dimensional collagen gels: effect of collagen concentration. *Biophys. J.* 61:306–315.

Patel, N., R. Padera, G. H. Sanders, S. M. Cannizzaro, M. C. Davies, R. Langer, C. J. Roberts, S. J. Tendler, P. M. Williams, and K. M. Shakesheff. 1998. Spatially controlled cell engineering on biodegradable polymer surfaces. *FASEB J.* 12:1447–1454.

Rich, A. M., and A. K. Harris. 1981. Anomalous preferences of cultured macrophages for hydrophobic and roughened substrata. *J. Cell Sci.* 50:1–7.

Richardson, R. R. J., J. A. Miller, and W. M. Reichert. 1993. Polyimides as biomaterials: preliminary biocompatibility testing. *Biomaterials.* 14: 627–635.

Saltzman, W. M., M. L. Radomsky, K. J. Whaley, and R. A. Cone. 1994. Antibody diffusion in human cervical mucus. *Biophys. J.* 66:508–515.

Smith, C. M. N., D. P. Tukey, D. Mundshenk, W. Krivit, J. G. White, J. E. Repine, and J. R. Hoidal. 1982. Filtration deformability of rabbit pulmonary macrophage. *J. Lab. Clin. Med.* 99:568–579.

Stein, M. D., J. M. Stevens, and D. N. Herndon. 1983. Defective neutrophil chemotaxis resulting from thermal injury: restoration of directed migration by increasing Boyden chamber filter pore size. *Clin. Immunol. Immunopathol.* 27:234–239.

Stenger, D. A., J. J. Hickman, K. E. Bateman, M. S. Ravenscroft, W. Ma, J. J. Pancrazio, K. Shaffer, A. E. Schaffner, D. H. Cribbs, and C. W. Cotman. 1998. Microlithographic determination of axonal/dendritic polarity in cultured hippocampal neurons. *J. Neurosci. Methods.* 82: 167–173.

Strzemienski, P. J., P. L. Sertich, D. D. Varner, and R. M. Kenney. 1987. Evaluation of cellulose acetate/nitrate filters for the study of stallion sperm motility. *J. Reprod. Fertil. Suppl.* 35:33–38.

Tai, H., and H. M. Buettner. 1998. Neurite outgrowth and growth cone morphology on micropatterned surfaces. *Biotech. Prog.* 14:364–370.

Tan, J., and W. M. Saltzman. 1999. Influence of synthetic polymers on neutrophil migration in three-dimensional collagen gels. *J. Biomed. Mater. Res.* 46:465–474.

Tan, J., H. Shen, K. L. Carter, and W. M. Saltzman. 2000. Controlling human polymorphonuclear leukocytes motility using microfabrication technology. *J. Biomed. Mater. Res.* 51:694–702.

Tucker, S. P., L. R. Melsen, and R. W. Compans. 1992. Migration of polarized epithelial cells through permeable membrane substrates of defined pore size. *Eur. J. Cell Biol.* 58:280–290.

Wessa, T., M. Rapp, and H. J. Ache. 1999. New immobilization method for SAW-biosensors: covalent attachment of antibodies via CNBr. *Biosensors Bioelectronic.* 14:93–98.

Wessels, D., H. Vawter-Hugart, J. Murray, and D. R. Soll. 1994. Three-dimensional dynamics of pseudopod formation and the regulation of turning during the motility cycle of *Dictyostelium. Cell. Motil. Cytoskel.* 27:1–12.